

Comparison of Randomly-oriented ZnO Nanorods and Butterfly-type ZnO Nanorod Bundles for Toluidine Blue Photocatalytic Degradation

A. C. CAKIR^a, P. GULOGLU^a, M. BILGIN^b, S. ERTEN-ELA^{a*}

^aEge University, Solar Energy Institute, 35100, Bornova-Izmir, Turkey

^bAksaray University, Engineering Faculty, Environmental Engineering Dept., Aksaray, Turkey

This paper is devoted to the decontamination of wastewater using ZnO nanostructures. The photocatalytic degradation of aqueous solution of a commercial dye, toluidine blue (TBO), has been investigated with two different kinds of ZnO nanostructures comprising butterfly-type ZnO nanorods and randomly-oriented ZnO nanorods. In order to be able to compare the photocatalytic efficiency, ZnO photocatalysts with two different crystalline structures are prepared by using different precursors but operating same microwave-assisted method. Butterfly-type ZnO nanorods are synthesized by using surfactants. Randomly-oriented ZnO nanorods with environmentally-friendly method are obtained without using any base and surfactant. The two different kinds of ZnO photocatalysts are characterized by X-Ray diffraction (XRD), scanning electron microscopy (SEM), UV-Vis absorption spectrum. The effects of pH, ZnO catalyst dosage and TBO initial dye concentration are tested experimentally for photocatalytic degradation. After 90 minutes reaction time, the decolorization efficiency of the TBO achieved 85.20% for butterfly-type ZnO nanorods and 77.20% for randomly-oriented ZnO nanorods. Additionally, under the same optimum conditions of pH=11, [ZnO]= 1g-ZnO L⁻¹, [TBO]= 108 mg TBO L⁻¹, Total Organic Carbon (TOC) removal efficiencies are obtained 56.70% and 40.80% for butterfly-type ZnO nanorods and randomly-oriented ZnO nanorods, respectively.

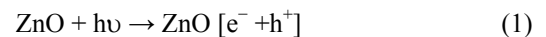
(Received February 3, 2012; accepted April 11, 2012)

Keywords: Decontamination of water, Photocatalysis, ZnO nanorod, Photodegradation, Total Organic Carbon Removal

1. Introduction

Industries such as plastic, textile, paper, rubber requires use of dyes widely. However, dyes give rise to the contamination due to the emitting of the toxic, cancerogenic and colored wastewater into water bodies [1-4]. Adsorption and chemical coagulation are the two common techniques of treatment of such wastewater [5]. But, the traditional techniques for the treatment of dye waste effluents are usually non-destructive, inefficient and costly or just transfer pollutants from water to another phase [6-11]. Advanced oxidation processes (AOPs) are alternative techniques of destruction of dyes and many other organics in wastewater and effluents. These processes generally involve UV/H₂O₂, UV/O₃ or UV/Fenton's reagent for the oxidative degradation of contaminants. Semiconductor photocatalysis is another developed advanced oxidation process, which can be conveniently applied to remove of different organic pollutants [5]. Moreover, this process utilizes cheaply available semiconductors and leads to complete mineralization of organic compounds to CO₂, water and mineral acids. Until now, many kinds of semiconductors have been studied as photocatalysts including TiO₂, ZnO, CdS, WO₃. Among them, nano-sized ZnO and TiO₂ as photocatalyst has been widely used for its high efficiency, non-toxic nature and low cost [12-17]. ZnO is a kind of semiconductor that has the similar band gap as TiO₂.

However, the greatest advantage of ZnO is that it absorbs large fraction of the solar spectrum and more light quanta than TiO₂ [18]. For this reason, ZnO photocatalyst is the most suitable for photocatalytic degradation in the presence of sun light. Photocatalytic process of ZnO is shown below.



The shape, crystalline structure and size of semiconductors are important factors in determining their physical and chemical properties. Rapid progress has been attained during recent years concerning preparation of ZnO nanostructures including nanowire [19], nanorods [20], nanoribbons [21], nanotubes [22], multipods [23], hollow spheres [24], sword-like nanowires [25] and flower shaped nanostructures [26] by various hydrothermal procedures [27], low-temperature chemical aqueous

solution [28], chemical vapor deposition (CVD) [29] and metal-organic CVD [30] methods. However, most of these methodologies are limited due to use of high temperature, high pressure, toxic reagents and long reaction time. Hence there is sufficient scope for the development of facile, rapid, convenient and additive free synthesis of nanocrystalline zinc oxide which can provide both qualitative and quantitative support for its commercial applications. Recently, microwave technique is extensively used for the synthesis of materials [31]. It has the advantages of homogeneous volumetric heating, high reaction rate and selectivity and energy savings as compared with conventional heating methods, making it promising for the synthesis of nanosized materials [32].

In this paper, two kinds of ZnO powder, butterfly-type ZnO nanorods and randomly-oriented ZnO nanorods using microwave-assisted preparation method are prepared by changing precursors. To our knowledge of literature, the use of butterfly-type ZnO nanorods for decontamination of water is a new concept and there is no paper or any report on photodegradation comprising the use of butterfly-type ZnO nanorods. Thus, this type of ZnO nanorods is synthesized and characterized newly and tested in photocatalytic experiments in this paper. This study deals with the comparative investigation of the photocatalytic degradation of TBO using two different morphologies of ZnO nanorods. The influence of size, morphology and also experimental parameters like initial dye concentration, catalyst loading, pH on the photocatalytic properties of ZnO powders are investigated. Both the removal of color and the removal of total organic carbon (TOC) are fully analysed. To understand the effect of two different kinds of ZnO nanorod photocatalysts, decolorization analysis and TOC removals are discussed.

2. Materials and Methods

2.1. Materials

Zinc acetate dihydrate $Zn[CH_3COO]_2 \cdot 2H_2O$, hexamethylenetetramine [HMT]; $[CH_2]_6N_4$, polyethyleneglycol 400 [PEG400], NaOH and HCl are purchased from Sigma-Aldrich. All chemicals used in this study are analytical grade and used directly without any further purifications. Deionized water is used for all experiments.

2.2. Preparation of Randomly-oriented ZnO nanorod Photocatalyst

In a typical experiment, zinc acetate is dissolved in 25 ml deionized water in a beaker. The solution is stirred with magnetic bar at 100 °C for 1 hour until a transparent mixture is obtained. The above solution is loaded into a 100 ml Teflon container. Then solution is irradiated by microwave energy using the microwave oven at 200 °C for 60 minutes [CEM MARS-5, frequency 2.45 GHz, maximum power 700 W, multimode oven]. Subsequently, the solution is loaded into a beaker and heated at 200 °C

until water evaporated. After wet precipitate is dried in an oven at 90 °C for 12 h. Finally, in order to obtain ZnO nanorods, white powder is calcined in a furnace at 200 °C for 36 hours.

2.3. Preparation of Butterfly-type ZnO nanorod photocatalyst

In this process, zinc acetate dihydrate $[Zn[CH_3COO]_2 \cdot 2H_2O]$ and HMT are used as Zn and OH⁻ sources. 1.1 g Zinc acetate dihydrate is dissolved in 25 ml deionized water in a beaker and then 0.7 g HMT and PEG400 is slowly added into the solution and stirred 30 minutes. Subsequently, solution is poured into a 100 ml of teflon container. The reaction mixture is heated in a microwave oven at a power of 300 W for 30 min. Then cooled at room temperature naturally. The material is filtered and washed with deionized water in order to remove impurities, dried at 70 °C for 12 h. Finally ZnO is annealed at 450 °C in order to obtain butterfly-type ZnO nanorod photocatalyst.

2.4. Randomly-oriented ZnO nanorod and butterfly-type ZnO nanorod photocatalysts characterization

The obtained samples are characterized on a Rigaku X-Ray diffractometer (XRD) with Cu K α radiation [1.540 Å]. The operation voltage and current are kept at 40 kV and 40 mA respectively. Scanning electron microscopy (SEM) images are obtained using a Philips XL 30S FEG. The photoluminescence spectra are recorded using a PTI-QM1 spectrophotometer. UV-VIS absorption spectra are performed on an analytic JENA S 600 UV-Vis spectrophotometer.

2.5. Photocatalytic experiment

By measuring photodegradation efficiency of toluidine blue with a definite concentration in an aqueous solution under illumination of UV, photocatalytic activity of two types of ZnO powders are evaluated. A solution containing known concentration of dye (TBO) and ZnO powder is prepared and it is equilibrated for 30 minutes in the dark. Then, 200 ml of prepared solution is transferred to 500 ml pyrex reactor. A 750 W UV Xe lamp is used a light source. Prior to each test, the lamp is turned on and warm up for about 10 minutes in order to get constant output. The distance between the solution and UV source is 10 cm and the temperature of the reaction is controlled at 22 °C by circulating water in all experiments. Subsequently, the mixture is poured into the photoreactor and began photocatalytic degradation tests. For investigating the effect of pH values on the photodegradation efficiency, the suspension pH values are adjusted at desired level using dilute NaOH and HCl. The photocatalytic activities of two different types ZnO powders are compared each other under the same

condition. Fig. 1 shows the schematic illustration of ZnO photodegradation mechanism and Molecular Structure of Toluidine Blue (TBO). During irradiation, the reaction solution is mixed by an air difusser, which is placed at the the reactor to uniformly disperse air into solution. Samples are collected at specific intervals and are immediately centrifuged to remove particles for analysis. The maximum absorbance intensity at wavelength of 632 nm is experimentally determined using a spectrophotometer and it is used to monitor the decolorization of toluidine blue. Total organic carbon (TOC) samples are fully analysed using a TOC analyzer. The degradation of the dyes in wastewater is defined as follows,

$$\eta = \frac{C_0 - C_t}{C_0} \times 100\%$$

where the η is the decolorization efficiency or TOC removal efficiency of dyes in wastewater, C_0 is the initial dye concentration or TOC concentration, the C_t is the dye concentration or TOC concentration at certain reaction time (t, minute).

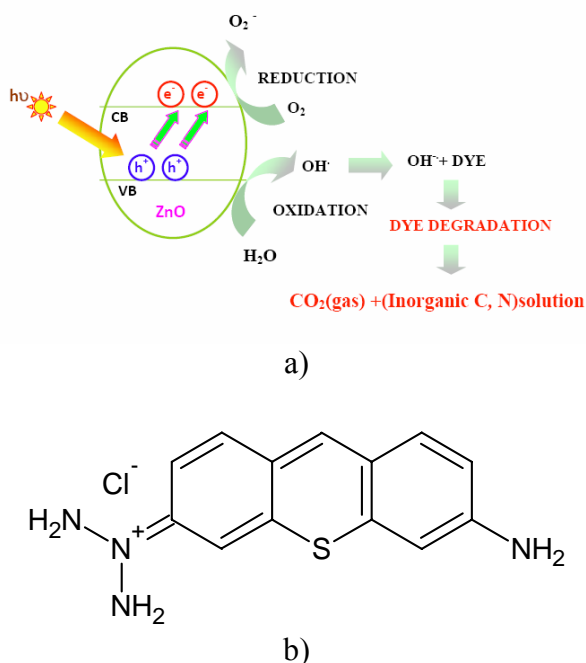


Fig. 1. Schematic illustration of ZnO photodegradation mechanism (a), Molecular Structure of Toluidine Blue (TBO) (b).

3. Results and discussion

3.1. Characterization of Photocatalysts

Fig. 2 illustrates the X-Ray diffraction pattern of the two different types ZnO nanorods. The XRD pattern

shows that all the diffraction peaks can be well indexed to those of the pure hexagonal wurtzite ZnO [S.G.: P63mc, with a polar c axis], and the lattice constants of the product is $a=0.324$ nm and $c=0.520$ nm. The diffraction peaks are in good agreement with the JCPDS card of wurtzite ZnO [JCPDS], No. 65-3411]. The clear and sharp diffraction peaks also indicate that the as-synthesized white ZnO products are highly crystallized. Impurities were not observed in the XRD pattern, confirming the high purity of the synthesized products.

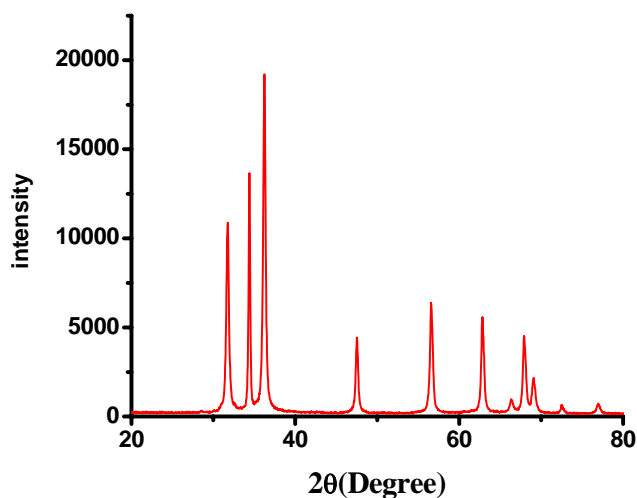


Fig. 2. XRD pattern of ZnO nanorods.

3.2. The Evaluation of photocatalytic degradation efficiencies of TBO using two kinds of ZnO nanorod photocatalysts

Scanning electron microscopy (SEM) is a powerful means to observe the morphology and crystalline structures of the nanorod products. We succeeded to observe the morphology of the products using SEM. Fig. 3 shows the SEM pictures of the products. It can be seen that the as-synthesized product consists of ZnO nanorods with relatively high density and random distribution in Fig. 3(a). The lengths of ZnO nanorods range from 600 nm to 950 nm and diameters range from 20-30 nm. The Fig. 3(b) shows the morphology and crystalline structures of butterfly-type ZnO nanorod bundles with length of 5 μ m approximately. The main parameter is crystal quality that pure crystalline structures give best efficiency in photocatalytic experiments. Both XRD and SEM results show that crystal qualities of ZnO nanostructures are so high to carry out the photocatalytic experiment in best efficiencies.

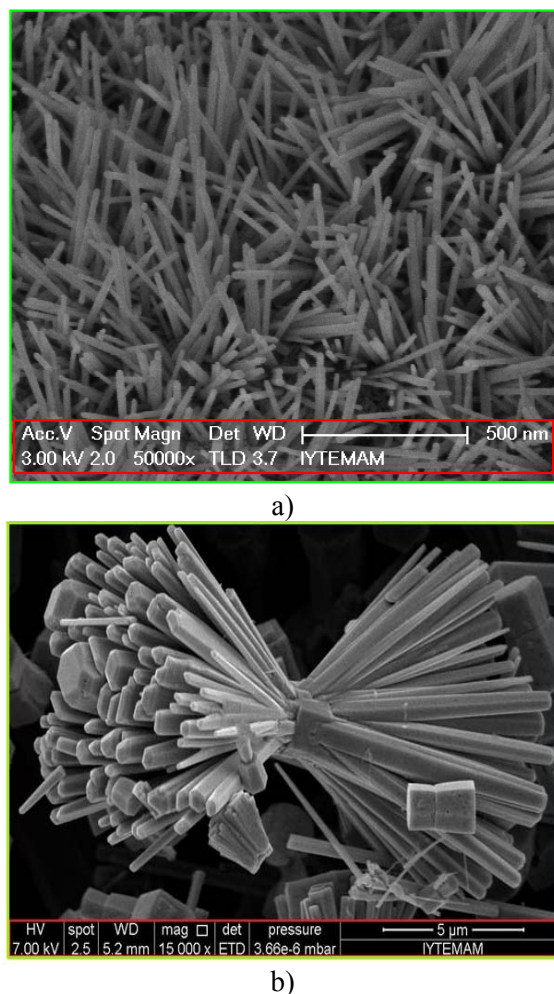


Fig.3. SEM images of two different types ZnO nanocrystalline structures; Randomly-oriented ZnO nanorods (a), butterfly-type ZnO nanorod bundles (b).

3.3. Effect of pH

The effect of pH on the photocatalytic activity of randomly-oriented ZnO nanorods and butterfly-type ZnO nanorod bundle photocatalysts are tested and the results are shown in Fig. 4. It can be seen that pH plays a crucial role in photocatalytic degradation that the photocatalytic activity of butterfly-type ZnO nanorod bundles shows an increase with the increasing pH from 3 to 11. The optimum pH is found to be as 11. Also, ZnO catalyst dosage and initial dye concentration of TBO are determined as $[\text{ZnO}] = 1.0 \text{ g.L}^{-1}$ and $[\text{TBO}] = 4 \times 10^{-4}$ (108 mg.L^{-1}), respectively. Decolorization efficiency of TBO is increased from 34% to 84% for butterfly-type ZnO nanorod bundles by increasing pH. And, decolorization efficiency of TBO is increased from 41% to 68% for randomly-oriented ZnO nanorods by increasing pH. Also results show that butterfly-type ZnO nanorods are more effective than randomly-oriented ZnO nanorods in photocatalytic experiments. The pH effect on the photocatalytic activity of the butterfly-type ZnO nanorod bundle and randomly-oriented ZnO nanorod

photocatalysts can be explained on the basis of the point of zero charge of ZnO. At a low pH, the surface of ZnO photocatalyst is positively charged, but at a high pH it becomes negatively charged. Since TBO is cationic dye, high pH favors the adsorption of TBO molecule on the catalyst surfaces which results in a high decolorization efficiency of TBO under neutral and basic conditions.

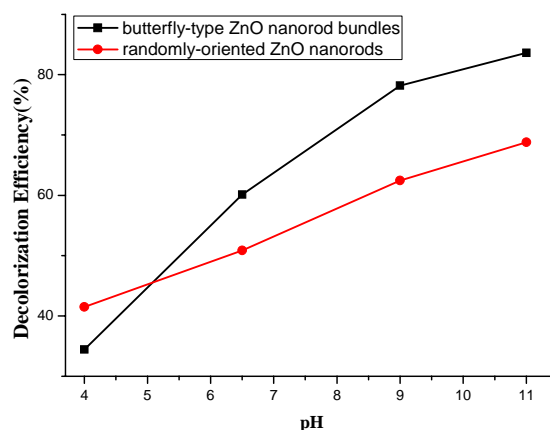


Fig. 4. Effect of pH on the photocatalytic activity of the butterfly-type ZnO nanorods and randomly-oriented ZnO nanorods photocatalyst. Experimental condition: $[\text{dye}] = 4 \times 10^{-4} \text{ M}$ (108 mg.L^{-1}), $[\text{ZnO}] = 1.0 \text{ g.L}^{-1}$, temperature = 22°C and reaction time = 90 min.

3.4. Effect of the catalyst dosage

Catalyst dosage is another important parameter in photocatalytic experiments. To test the effects of catalyst dosages on the photocatalytic degradation of Toluidine Blue (TBO), we carried out lots of experiments and the results are shown in Fig. 5 and Fig. 6 for randomly-oriented ZnO nanorods and butterfly-type ZnO nanorod bundles. It can be seen that the decolorization efficiency of TBO increases from 40.80% to 85.20% by increasing the dosage of ZnO photocatalyst from 0.5 to 1.0 g.L^{-1} for butterfly-type ZnO nanorods and from 72.87% to 77.15% for randomly-oriented ZnO nanorods. This is because of increasing catalyst dosage, the photogenerated electron hole pairs and HO^\bullet are correspondingly increased, which lead to more dye molecules degradation. When the catalyst dosages increase from 1.0 g.L^{-1} to 1.5 g.L^{-1} , we observed that the decolorization efficiencies decrease from 77.15% to 63.20% and from 85.20% to 18.40% for additive-free ZnO and butterfly-type ZnO nanorod bundles, respectively. These results show that degradation efficiency of TBO does not increase by increasing catalyst dosages. Also this effect can be explained by the fact that when the catalyst dosage of ZnO is too much, it effects the solution's transparency and causes a scattering effect. Thus it reduces the light utilization rate and lower the photocatalytic activity of ZnO nanorod photocatalysts. Therefore, the results show that an optimum dosage of ZnO photocatalysts for the degradation of TBO is 1.0 g.L^{-1} .

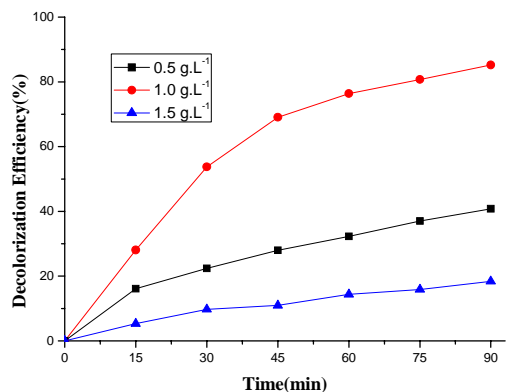


Fig. 5. Effect of catalyst dosage on the photocatalytic degradation of TBO by the butterfly-type ZnO photocatalyst. Experimental conditions: [dye] = pH 11, temperature = 22 °C.

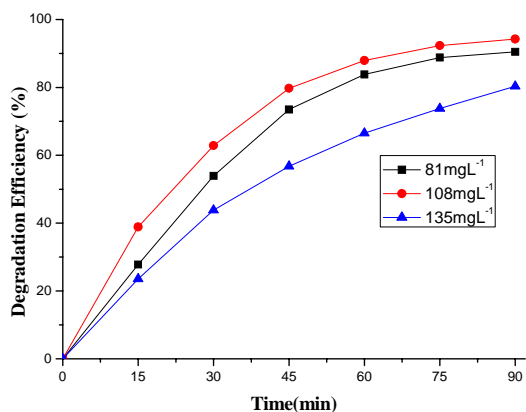


Fig. 7. Effect of initial dye concentration on the photocatalytic degradation of TBO by the butterfly-type ZnO photocatalyst. Experimental conditions: pH 11, [ZnO] = 1.0 gL⁻¹, temperature = 22 °C

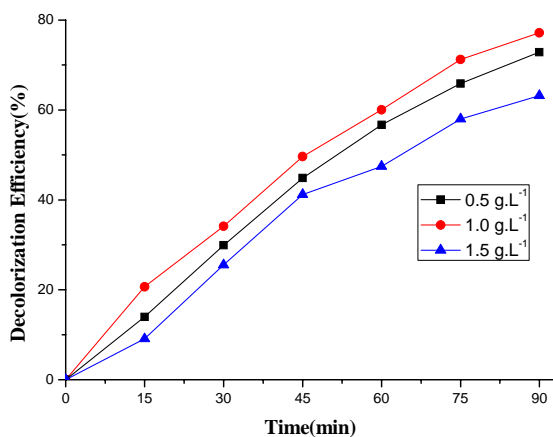


Fig. 6. Effect of catalyst dosage on the photocatalytic degradation of TBO by the randomly-oriented ZnO photocatalyst. Experimental conditions: [dye] = 4 × 10⁻⁴ M (108 mg L⁻¹), pH 11, temperature = 22 °C.

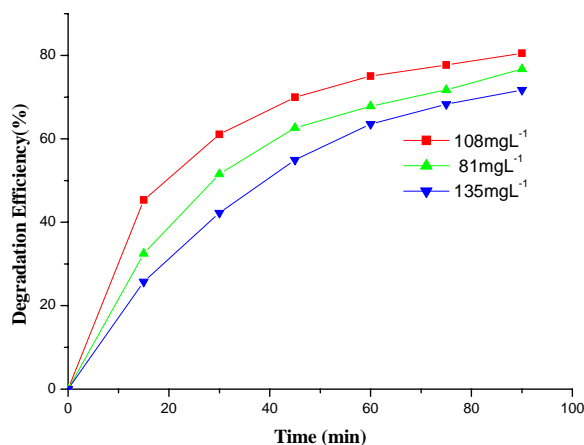


Fig. 8. Effect of initial dye concentration on the photocatalytic degradation of TBO by the randomly-oriented ZnO photocatalyst. Experimental conditions: pH 11, [ZnO] = 1.0 gL⁻¹, temperature = 22 °C

3.5. Effect of initial concentration of TBO

The effect of initial concentration of TBO on the photocatalytic degradation efficiency is tested by varying the initial concentration of TBO from 3.10⁻⁴–5.10⁻⁴ M (81–135 mgL⁻¹), the results are shown in Fig. 7 and Fig. 8.

The results show that the decolorization efficiency of TBO is strongly depended on the initial dye concentration. The decolorization efficiency of TBO increased from 90.50% to 94.25% and 76.74% to 80.52% for butterfly-type ZnO nanorod bundles and randomly-oriented ZnO nanorods, respectively by increasing of the initial dye concentration from 3.10⁻⁴ M to 4.10⁻⁴ M (from 81 to 108 mgL⁻¹).

However, the decolorization efficiency of TBO decreases from 94.25% to 80.35% and 80.52% to 71.70% for butterfly-type ZnO nanorod bundles and randomly-oriented ZnO nanorods, respectively by increasing of initial dye concentration from 4.10⁻⁴ to 5.10⁻⁴ M (from 108 to 135 mgL⁻¹), respectively. We can explain this effect that high concentrated dye solution decrease the light utilization rate by ZnO photocatalysts. As a result of this effect, photodegradation of TBO decreases by increasing initial dye concentrations. The optimum TBO concentration is found to be as 4.10⁻⁴ M (108 mgL⁻¹).

3.6. Comparison of photocatalytic activity of the randomly-oriented ZnO nanorods and butterfly-type ZnO nanorod bundles

Fig. 9 shows the comparison of the decolorization and TOC removal efficiencies of TBO in aqueous solution of randomly-oriented ZnO nanorods and butterfly-type ZnO nanorod bundles for 1.0 gL^{-1} ZnO photocatalyst dosages. It can be seen that the TOC removal efficiency of TBO is 40.80% for 1.0 gL^{-1} randomly-oriented ZnO nanorod photocatalyst. And the TOC removal efficiency of TBO is 56.70% for 1 gL^{-1} butterfly-type ZnO nanorod bundles after 90 minutes reaction time. The decolorization efficiency of TBO is 77.20% for 1.0 gL^{-1} randomly-oriented ZnO nanorod photocatalyst. And the decolorization efficiency of TBO is 85.20% for 1.0 gL^{-1} butterfly-type ZnO nanorod bundles after 90 minutes reaction time.

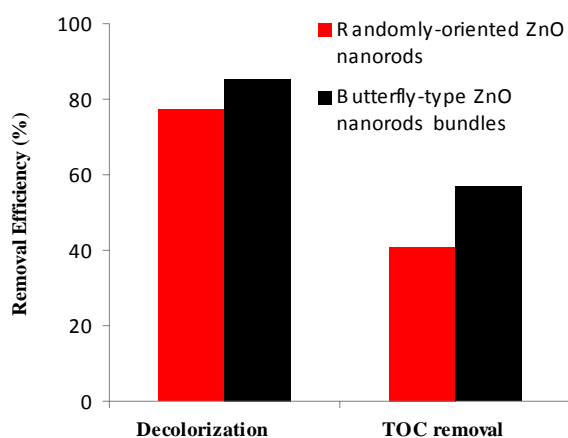


Fig. 9. Removal TOC efficiency (%) and Decolorization efficiency (%) using two kinds of ZnO photocatalysts in photocatalytic experiment..

The results above indicate that the butterfly-type ZnO nanorod bundle photocatalyst shows a good photocatalytic activity under optimum conditions ($\text{pH}=11$, $[\text{ZnO}]=1 \text{ g-ZnO L}^{-1}$, $[\text{TBO}]=108 \text{ mg TBO L}^{-1}$), which might be attributed to its unique microstructure to absorb a large fraction of UV light. Because, the length of butterfly-type ZnO nanorod is $5 \mu\text{m}$ approximately. The surface area of butterfly-type ZnO nanorod is bigger than randomly-oriented ZnO nanorods. The surface area, pH, TBO and ZnO concentration are important parameters for the photocatalytic degradation of TBO. On contrary, the agglomeration of randomly-oriented ZnO nanoparticles decreases the UV light utilization rate, which reduces its photocatalytic activity and results in a low decolorization efficiency of TBO.

3.7. Kinetic analysis

In the present study, it is found that the photocatalytic degradation of TBO by the butterfly-type ZnO nanorod bundles photocatalyst is obeyed the pseudo-first-order

kinetics. The pseudo-first-order kinetics for TBO's degradation is calculated as follows (Eq.(2) and Eq.(3)):

$$-\frac{dC}{dt} = kC \quad (2)$$

$$\ln\left(\frac{C_0}{C}\right) = kt \quad (3)$$

where k is the pseudo-first-order rate constant (min^{-1}), C_0 is the initial concentration of TBO (mg L^{-1}), C is the concentration of TBO at reaction time (t , minute). The linear plots of $\ln(C_0/C)$ versus irradiation time (t , minute) are shown in Fig. 10 and Fig. 11. In principle, the photocatalytic degradation of TBO by the ZnO photocatalyst is an interface process, which might follow the Langmuir-Hinshelwood model (Eq. (4) and Eq.(5)):

$$r_0 = -\frac{dC}{dt} = \frac{K_1 K_2 C}{1 + K_2 C_0} = k_{ap} C \quad (4)$$

$$\frac{1}{k_{ap}} = \frac{1}{K_1 K_2} + \frac{C_0}{K_1} \quad (5)$$

where C_0 is the initial concentration of TBO (mgL^{-1}), K_1 is the surface reaction rate constant ($\text{mgL}^{-1}\text{min}^{-1}$), K_2 is the Langmuir-Hinshelwood adsorption equilibrium constant (Lmg^{-1}) and k_{ap} (min^{-1}) is the the pseudo-first-order rate constant. A plot of $1/k_{ap}$ and dye concentration was observed ($R=0.9986$ and 0.9449), which indicated that the photocatalytic degradation of TBO by the butterfly-type ZnO nanorod bundles photocatalyst followed the Langmuir-Hinshelwood model (Fig. 12 and Fig. 13).

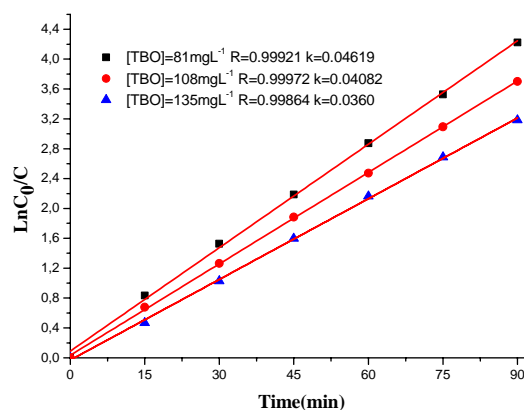


Fig. 10. The plots of $\ln C_0/C$ versus reaction time (t , min) with different initial concentrations of TBO for butterfly-type ZnO nanorods. Experimental conditions: $[\text{dye}] = 4 \times 10^{-4} \text{ M}$ (108 mg L^{-1}), $\text{pH} 11.0$, $[\text{ZnO}] = 1.0 \text{ g L}^{-1}$, temperature = 22°C .

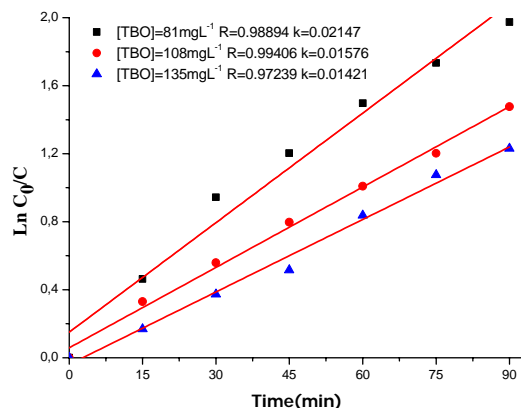


Fig. 11. The plots of $\ln C_0/C$ versus reaction time (t, min) with different initial concentrations of TBO for randomly-oriented ZnO nanorods. Experimental conditions: $[\text{dye}] = 4 \times 10^{-4} \text{ M}$ (108 mg L^{-1}), $\text{pH } 11.0$, $[\text{ZnO}] = 1.0 \text{ g L}^{-1}$, temperature = 22°C .

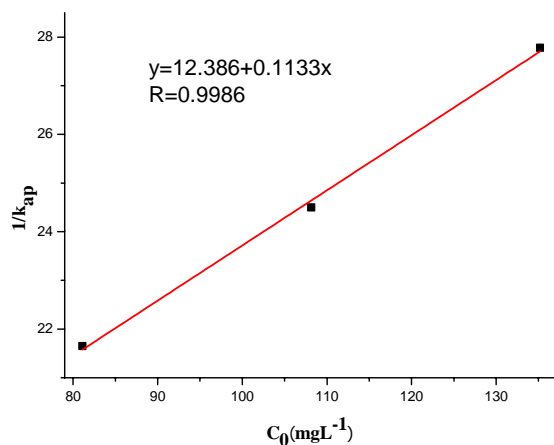


Fig. 12. The relationship between the $1/k_{ap}$ and the initial concentration of TBO for butterfly-type ZnO nanorods. Experimental conditions: $[\text{dye}] = 4 \times 10^{-4} \text{ M}$ (108 mg L^{-1}), $\text{pH } 11$, $[\text{ZnO}] = 1.0 \text{ g L}^{-1}$, temperature = 22°C and reaction time = 90 min.

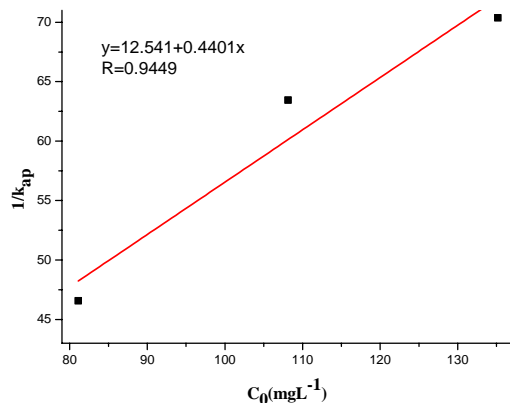


Fig. 13. The relationship between the $1/k_{ap}$ and the initial concentration of TBO for randomly-oriented ZnO nanorods. Experimental conditions: $[\text{dye}] = 4 \times 10^{-4} \text{ M}$ (108 mg L^{-1}), $\text{pH } 11$, $[\text{ZnO}] = 1.0 \text{ g L}^{-1}$, temperature = 22°C and reaction time = 90 min.

4. Conclusion

In this study, randomly-oriented ZnO nanorods and butterfly-type ZnO nanorods are successfully synthesized by microwave-heating method. Butterfly-type ZnO nanorods are firstly tested experimentally for photocatalytic degradation in literature. It is found that pH is an important factor for photocatalytic degradation of TBO using butterfly-type ZnO nanorods. The decolorization efficiency and TOC removal efficiency of butterfly-type ZnO nanorods after 90 minutes reaction time are successfully achieved 85.20% and 56.70%, respectively.

Acknowledgement

We acknowledge support from TUBITAK (Scientific and Technological Research Council of Turkey) and Alexander von Humboldt Foundation. I thank Mechanical Engineer MSc. Cagatay ELA for his valuable advices, support and proofreading.

References

- [1] A. Houas, H. Lachheb, M. Ksibi, E. Elaloui, C. Guillard, J.M. Herrmann, *Appl. Catal. B: Environ.* **31**, 145 (2001).
- [2] I.K. Konstantinou, T.A. Albanis, *Appl. Catal. B: Environ.* **49**, 1 (2004).
- [3] P.A. Pekakis, N.P. Xekoukoulotakis, D. Mantzavinos, *Wat. Res.* **40**, 1276 (2006).
- [4] L.Y. Yang, S.Y. Dong, J.H. Sun, J.L. Feng, Q.H. Wu, S.P. Sun, *J. Hazard. Mater.* **179**, 438 (2010).
- [5] S. Chakrabarti, B.K. Dutta, *J. Hazard. Mater.* **112**, 269 (2004).
- [6] A. Abdel Aal, S.A. Mahmoud, A.K. Aboul-Gheit, *Mat. Sci. Eng. C* **29**, 831 (2009).
- [7] N. Daneshvar, D. Salari, A.R. Khataee, *J. Photochem. Photobio. A: Chem.* **162**, 317 (2004).
- [8] A. Criscoli, J. Zhong, A. Figoli, M.C. Carnevale, R. Huang, E. Drioli, *Wat. Res.* **42**, 5031 (2008).
- [9] M. Constapel, M. Schellentrager, J.M. Marzinkowski, S. Gáb, *Wat. Res.* **43**, 733 (2009).
- [10] V. Meshko, L. Markovska, M. Mincheva, A.E Rodrigues, *Wat. Res.* **35**, 3357 (2001).
- [11] F. Harrelkas, A. Azizi, A. Yaacoubi, A. Benhammou, M.N. Pons, *Desalination* **235**, 330 (2009).
- [12] J. Wang, Z. Jiang, Z. Zhang, Y. Xie, X. Wang, Z. Xing, R. Xu, X. Zhang, *Ultrason. Sonochem.* **15**, 768 (2008).
- [13] B. Liu, T. Torimoto, H. Yoneyama, *J. Photochem. Photobio. A: Chem.* **113** (1998) 93–97.
- [14] I. Konstantinou, T. Sakellariades, V. Sakkas, T. Albanis, *Environ. Sci. Technol.* **35**, 398 (2001).
- [15] Y.T. Kwon, K.Y. Song, W.I. Lee, G.J. Choi, Y.R. Do, *J. Catal.* **191**, 192 (2000).

- [16] H. Lin, S. Liao, S. Hung, J. Photochem. Photobio. A: Chem. **174**, 82 (2005).
- [17] H. Wang, C. Xie, W. Zhang, S. Cai, Z. Yang, Y. Gui, J. Hazard. Mat. **141**, 645 (2007).
- [18] S. Sakthivel, B. Neppolian, M.V. Shankar, B. Arabindoo, M. Palanichamy, V. Murugesan, Sol. Energy Mater. Sol. Cells **77**, 65 (2003).
- [19] Y. Guo, H. Wang, He C., L. Qiu, X. Cao, Langmuir **25**, 4678 (2009).
- [20] a) S. Erten-Ela, S. Cogal, G. Turkmen, S. Icli, Current Appl. Phys. **10**, 187 (2010); b) S. Erten-Ela, S. Cogal, S. Icli, Inorg. Chim. Acta **362**, 1855 (2009); c) S. Erten-Ela, S. Cogal, S. Icli, Optoelectron. Adv. Mater. Rapid Comm. **3**, 459 (2009); d) D. Rana Bekci, S. Erten-Ela, Renewable Energy **43**, 378 (2012).
- [21] X.Y. Kong, Z.L. Nano Lett. **3**, 1625 (2003).
- [22] H. Yu, Z. Zhang, M. Han, X. Hao, F. Zhu, J. Am. Chem. Soc. **127**, 2378 (2005).
- [23] H. Yan, R. He, J. Pham, P. Yang, Adv. Mater. **15**, 402 (2003) -405.
- [24] M. Mazloumi, S. Taghavi, H. Arami, S. Zanganeh, A. Kajbafvala, M.R. Shayegh, S.K. Sadrnezhad, J. Alloy Compd. **468**, 303 (2009).
- [25] T. Thongtema, A. Phuruangratb, S. Thongtem, Ceram. Int. **36**, 257 (2010) .
- [26] H. Zhang, J.Y. Xiangyang, J. Xu, D. Que, D. Yang, Nanotechnology **15**, 622 (2004).
- [27] B. Cheng, E.T.Samulski, Chem. Comm. **10**, 986 (2004).
- [28] P. Li, Y. Wei, H. Liua, X. Wang, Chem. Comm. **24**, 2856 (2004) .
- [29] C.L. Wu, C. Li, H.G. Chen, C.W. Lin, C.W., T.F. Chang, Y.C. Chao, J.K. Yan, Thin Solid Films **498**, 137 (2006) .
- [30] J.Y. Park, H. Oh, J.J. Kim, S.S. Kim, J. Cryst. Growth **287**, 145 (2006).
- [31] K.D. Bhatte, P. Tambade, S.I Fujita, M. Arai, B.M. Bhanage, Powder Technol. **203**, 415 (2010).
- [32] P. Zhu, J. Zhang, Z. Wu, Z. Zhang, Crystal Growth & Design **8**, 3148 (2008).

*Corresponding author: suleerten@yahoo.com,
sule.erten@ege.edu.tr